Colloid Polym Sci (2007) 285:1515–1520
DOI 10.1007/s00396-007-1720-y

SHORT COMMUNICATION

Fabrication and characterization of TiO_2–SiO_2 composite nanoparticles and polyurethane/(TiO_2–SiO_2) nanocomposite films

Li Chen · Haixia Shen · Zhen Lu · Cang Feng · Su Chen · Yanru Wang

Received: 6 May 2007 / Revised: 24 May 2007 / Accepted: 11 June 2007 / Published online: 21 July 2007

Abstract TiO_2–SiO_2 composite nanoparticles were prepared by a sol–gel process. To obtain the assembly of TiO_2–SiO_2 composite nanoparticles, different molar ratios of Ti/Si were investigated. Polyurethane (PU)/(TiO_2–SiO_2) hybrid films were synthesized using the "grafting from" technique by incorporation of modified TiO_2–SiO_2 composite nanoparticles building blocks into PU matrix. Firstly, 3-aminopropyltriethysilane was employed to encapsulate TiO_2–SiO_2 composite nanoparticles' surface. Secondly, the PU shell was tethered to the TiO_2–SiO_2 core surface via surface functionalized reaction. The particle size of TiO_2–SiO_2 composite sol was performed on dynamic light scattering, and the microstructure was characterized by X-ray diffraction and Fourier transform infrared. Thermogravimetric analysis and transmission electron microscopy (TEM) employed to study the hybrid films. The average particle size of the TiO_2–SiO_2 composite particles is about 38 nm when the molar ratio of Ti/Si reaches to1:1. The TEM image indicates that TiO_2–SiO_2 composite nanoparticles are well dispersed in the PU matrix.

Keywords TiO_2–SiO_2 composite nanoparticles · Ti–O–Si bond · Polyurethane/(TiO_2–SiO_2) nanocomposite hybrids

Introduction

In recent years, inorganic–organic hybrid materials have attracted considerable attention because of their outstanding chemical and physical properties [1]. The hybrid materials are applied in many fields, such as optical wave guide [2], semiconductor nanocrystals [3], magnetic materials [4], and bioactive materials [5]. The progress in new polymer synthesis techniques makes it possible to synthesize well-defined polymer–nanoparticle hybrids with novel properties and controlled architectures. There are many methods for attaching polymer chains onto nanoparticle surfaces, including chemisorption [6], covalent attachment of end-functionalized polymers to a reactive surface ("grafting to") [7], and in situ monomer polymerization with monomer growth of polymer chains from immobilized initiators ("grafting from") [8, 9]. Current polymerization methods used to prepare inorganic–organic hybrids by tethering the polymer chain to the nanoparticle surface include anionic, cationic, ring-opening metathesis, nitroxide-mediated, atom transfer radical polymerization, and reversible addition fragmentation chain transfer. During these polymerization procedures, the sol–gel [10–13] process is a common way because it has provided good opportunities for preparing inorganic–organic hybrid materials at the molecular level and the experimental condition is mild and easy to control.

Of these nanocomposite hybrids, polyurethanes (PUs), as the organic matrix, have provided a wide range of properties from a variety of starting materials. Tailor-made properties of these materials can be obtained from well-designed combinations of monomeric materials. On a molecular basis, PU may be described as the linear structure block copolymer of the $(AB)_n$ type. Part A, the hard segment, is composed of oligomers, which are prepared by the reaction of a low molecular weight diol or triol chain extender with diisocyanate. Part B, the soft segment, is normally a polyester or a polyether polyol with a molecular weight of 1,000–2,000. To improve the performance of PUs in various applications, PU nanocomposite hybrids and

L. Chen · H. Shen · Z. Lu · C. Feng · S. Chen (✉) · Y. Wang
College of Chemistry and Chemical Engineering,
Nanjing University of Technology,
No. 5 Xin Mofan Rd.,
Nanjing 210009, People's Republic of China
e-mail: chensu@njut.edu.cn

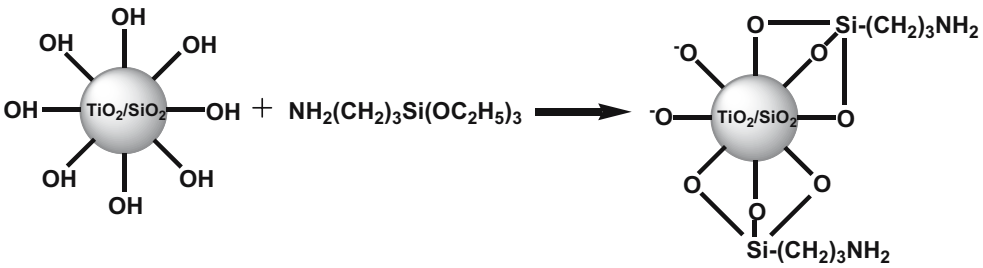

Scheme 1 Schematic formation of APTS/(TiO_2–SiO_2) composite nanoparticles

multiphase polymeric systems such as interpenetrating networks (IPNs) have been extensively used for more than three decades. Hideki and Curtis [14] prepared PU/SiO_2 hybrid films at the molecular level by a sol–gel process using the IPNs technique. Takavuki et al. [15] prepared PU/TiO_2 hybrid materials by a sol–gel process using triethoxysilyl end-capped urethane prepolymer and titanium isopropoxide. Chen et al. [16] studied the effects of different titania sol on the microstructure and properties of the PU/TiO_2 hybrid films. They found that the introduction of TiO_2 nanoparticles into the PU matrix could increase some physical properties such as viscosity, modulus, mechanical strength, abrasion resistance, hardness, and ultraviolet absorbance. Although many approaches have been done on PU/SiO_2 and PU/TiO_2 hybrid films [17–20], the reports on PU/(TiO_2–SiO_2) nanocomposite hybrid films have not been seen elsewhere.

Our preliminary investigations in the incorporation of an inorganic network such as the nanosilica phase into the PU matrix have been presented in a previous paper [21]. In this work, we report that the fabrication of TiO_2–SiO_2 nanoparticles and PU/TiO_2–SiO_2 nanocomposite films can be carried out by incorporating TiO_2–SiO_2 nanoparticles building blocks into the PU matrix. In pursuit of this, dynamic light scattering (DLS), X-ray diffraction (XRD), Fourier transform infrared spectroscopy (FT-IR), thermogravimetric analysis (TGA), and transmission electron microscopy (TEM) were employed for the characterization.

Experimental section

Materials

Tetrabutyl titanate (TBOT), ethyl silicate (TEOS), toluene 2,4-diisocyanate (TDI), and 3-aminopropyltriethoxysilane (APTS) were all of analytical-grade purity and were used as received. Ethanol was purified by a 4-Å molecular sieve and distilled under reduced pressure before use. Hydrochloric acid and ammonia water were used to control the pH value of the sol. 1,4-Butanediol (BD) and poly (propylene glycol) (hydroxyl number is 56 mg of KOH/g of N220, the average molecule weight of 2,000) were purged by distillation under reduced pressure before use. Toluene was used without further purification. Stannous caprylate was used as the catalyst for the preparation of PU.

Synthesis of TiO_2–SiO_2 nanoparticles

TiO_2–SiO_2 nanoparticles were synthesized by a sol–gel process with TBOT and TEOS (the molar ratio of Ti/Si

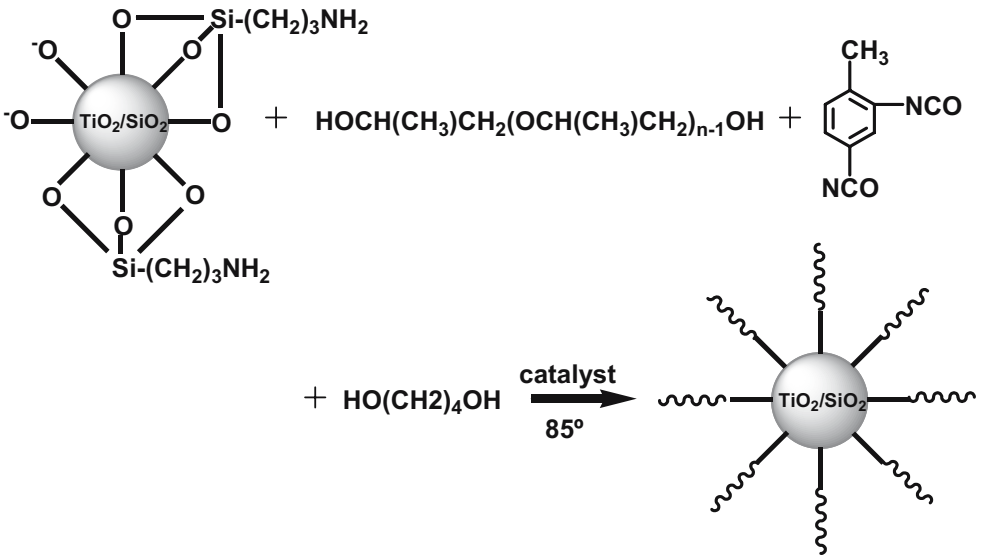

Scheme 2 Schematic formation of PU/(TiO_2–SiO_2) nanocomposite hybrids

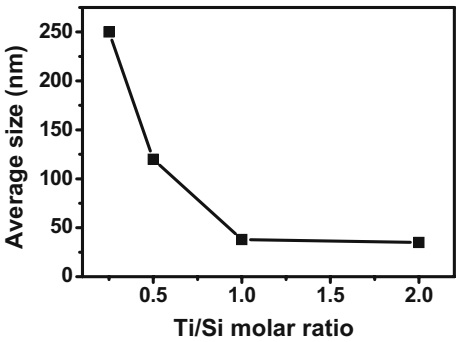

Fig. 1 The average size of different molar ratios of TiO_2/SiO_2 sol

ranged from 1/4 to 1/0.25) and 15 g ethanol carried out in a 250-ml conical flask with magnetic stirring at ambient temperature. In the first step, the solution of distilled water, hydrochloric acid, and 15 g ethanol was mixed well. Then, the mixture of TBOT and TEOS was added dropwise to this solution with a lower speed. The process was carried out under continuous magnetic stirring. In the second step, the TiO_2–SiO_2 nanocomposite sol was aged at room temperature for several days, then dried at 90 °C for 5 h. Finally, The gel of TiO_2–SiO_2 composite nanoparticles was calcinated by a muffle furnace at 500–550 °C for 3 h, and then TiO_2/SiO_2 nanoparticles were obtained.

Synthesis of polyurethane/TiO_2–SiO_2 nanocomposite hybrid films

In a typical run, 0.5 g TiO_2–SiO_2 composite nanoparticles in 40 g of toluene were refluxed with stirring at 110 °C for 2 h, and then 0.2 g APTS was added to this solution. The mixture was refluxed with vigorous stirring for 6 h. After isolation and dehydration with methanol washing, the free APTS was removed. Finally, the APTS-g–TiO_2–SiO_2 nanopowder was dried in vacuum oven. The schematic APTS grafted into TiO_2–SiO_2 nanoparticles' surface was

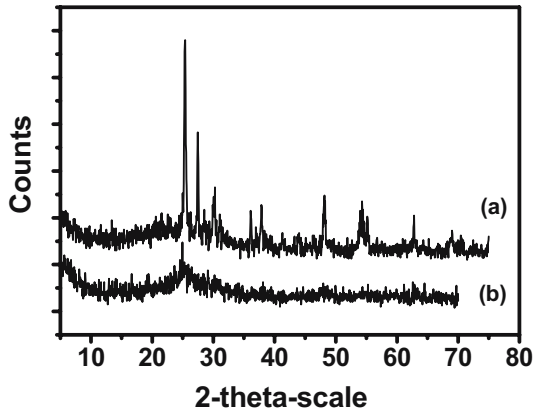

Fig. 3 XRD spectras of *a* mixture particles of TiO_2–SiO_2 (Ti/Si= 1:1 mol/mol; TiO_2–SiO_2-mixed gel was calcined at 500 °C) and *b* TiO_2–SiO_2 composite particles (Ti/Si=1:1 mol/mol; TiO_2–SiO_2 gel was calcined at 500 °C)

shown in Scheme 1. For synthesis of PU/(TiO_2–SiO_2) hybrids, firstly, the APTS-g–(TiO_2–SiO_2) nanopowder was dispersed in 40 g of toluene with continuously stirring. Then, 8.4 g TDI, 40 g PPG, and 1.8 g BD were introduced into the flask, where BD was used as a chain extender. The polymerization was carried out at 85 °C for 4 h. Finally, PU/TiO_2–SiO_2 nanocomposite hybrids were obtained. The schematic synthesis PU/(TiO_2–SiO_2) nanocomposite hybrids were shown in Scheme 2.

Characterizations

The particle size of TiO_2–SiO_2 sol was performed on a Malvern 3000 DLS. The XRD patterns were recorded on a Bruker-AXS D8 ADVANCE (Bruker, Germany) X-ray diffractometer at a scanning rate of 6 °/min in 2θ ranging from 1 ° to 80 ° with CuKα radiation. FT-IR (Nicolet-Nexus 670) spectroscopy was used to affirm the bond of Ti–O–Si. The morphologies of the nanocomposite hybrids

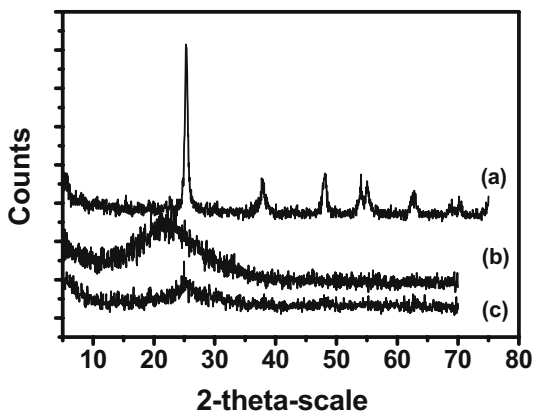

Fig. 2 XRD spectra of *a* pure TiO_2, *b* pure SiO_2, and *c* TiO_2–SiO_2 hybrid particles (Ti/Si=1:1 mol/mol; TiO_2–SiO_2 gel was calcined at 500 °C)

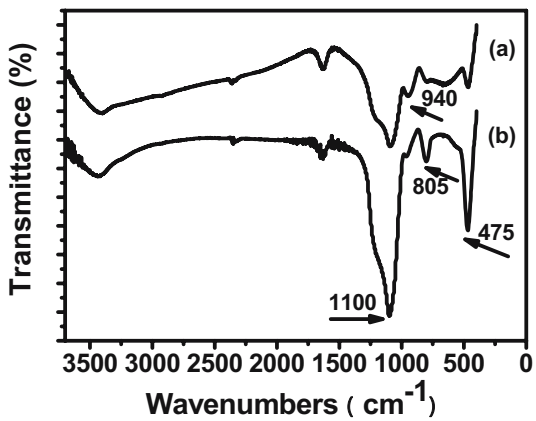

Fig. 4 FT-IR spectra of *a* TiO_2–SiO_2 composite nanoparticles (Ti/Si= 1/1 mol/mol; TiO_2–SiO_2 gel was calcinated at 500 °C; 3 h) and *b* pure SiO_2

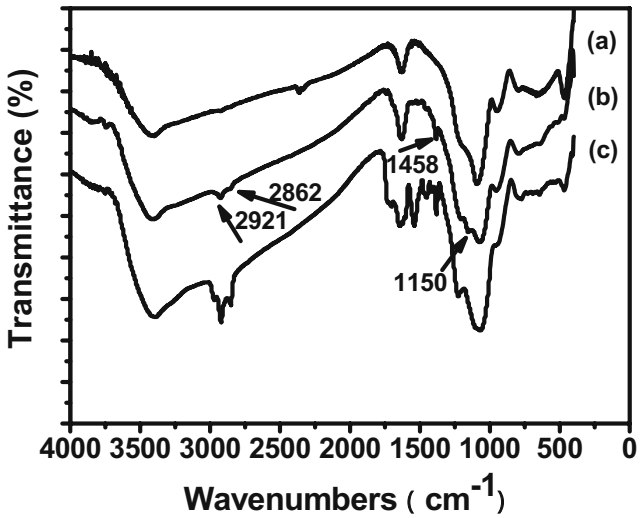

Fig. 5 FT-IR spectra of *a* TiO_2–SiO_2 composite nanoparticles (Ti/Si= 1/1 mol/mol; TiO_2–SiO_2 gel was calcinated at 500 °C; 3 h), *b* APTS/ TiO_2–SiO_2 hybrid particles (APTS/(TiO_2–SiO_2)=2 wt%), and *c* PU/ (TiO_2–SiO_2) particles washed by methanol and acetone ([NCO]/[OH]= 1.3/1.0 mol/mol; APTS/(TiO_2–SiO_2)=2 wt%; toluene=70 wt%)

were measured by TEM (Hitachi H-600). Thermal decomposition of the hybrid films was determined by TGA (Shimadzu TGA-50) where the heating rate was 10 °C/min in N_2 flow.

Results and discussion

DLS characterization of TiO_2–SiO_2 sol

Controlling the amount of TBOT and TEOS with various Ti/Si molar ratios in hybrid sol resulted in the change of the average particle size. As shown in Fig. 1, the average particle size of the hybrid sol presents a notable decrease with the increasing of Ti/Si molar ratio. When the Ti/Si molar ratio reaches to 1, the average particle size of the hybrid sol is 38 nm. Meanwhile, increasing the molar ratio continuously, the particle size of the hybrid sol changes a little. This may be because the TBOT precursor of TiO_2 hydrolyzes more quickly than that of TEOS. When the molar ratio of Ti/Si is more than 1:1, TiO_2 networks will encapsulate SiO_2 and limit the mass transportation of SiO_2, resulting in the production of smaller particle sizes of TiO_2/ SiO_2 composite nanoparticles.

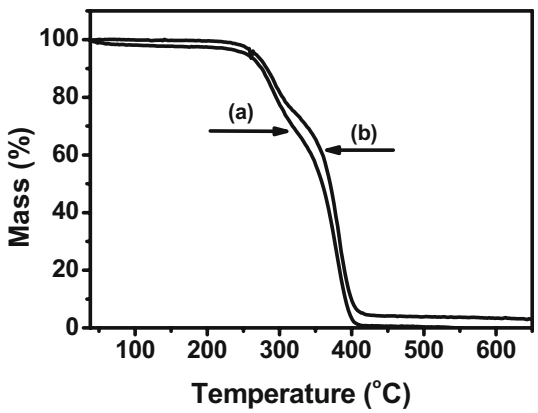

Fig. 6 TGA curves of *a* pure PU ([NCO]/[OH]=1.3/1.0 mol/mol; toluene=70 wt%) and *b* PU/(TiO_2–SiO_2) hybrids ([NCO]/[OH]=1.3/ 1.0 mol/mol; APTS/(TiO_2–SiO_2)=2 wt %; toluene=70 wt%)

XRD characterization of TiO_2–SiO_2 nanoparticles

The XRD patterns of pure TiO_2, pure SiO_2, and TiO_2–SiO_2 composite particles calcinated at 500 °C are presented in Fig. 2, respectively. As is seen in Fig. 2, the XRD pattern of pure TiO_2 (seen in Fig. 2a) shows obvious peaks at about 25.3 °, 37.8 °, 48.14 °, and 55 °, which are attributed to the characteristic peaks of anatase TiO_2. The XRD pattern of pure SiO_2 (seen in Fig. 2b) exhibits a broad amorphous peak at about 22 °, while there is a broad peak to occur at about 25 ° in Fig. 2c, implying that the XRD pattern of TiO_2–SiO_2 composite nanoparticles has a less-ordered structure. This may be attributed to the formation of Ti–O–Si bonds, limiting the growth of TiO_2 crystals. To seek further evidence of the existence of Ti–O–Si bonds, TiO_2–SiO_2 composite nanoparticles calcinated at 500 °C, along with the physical mixture of the TiO_2 gel and SiO_2 gel for comparison, were investigated by XRD as shown in Fig. 3. Both molar ratios of Ti/Si in Fig. 3 are all 1:1. The XRD results show that the XRD pattern of the mixture of the TiO_2 gel and SiO_2 gel is similar to that of TiO_2, while the XRD pattern of TiO_2–SiO_2 composite nanoparticles is amorphous. Therefore, a conclusion could be drawn that the Ti–O–Ti bonds were destroyed because of the phase

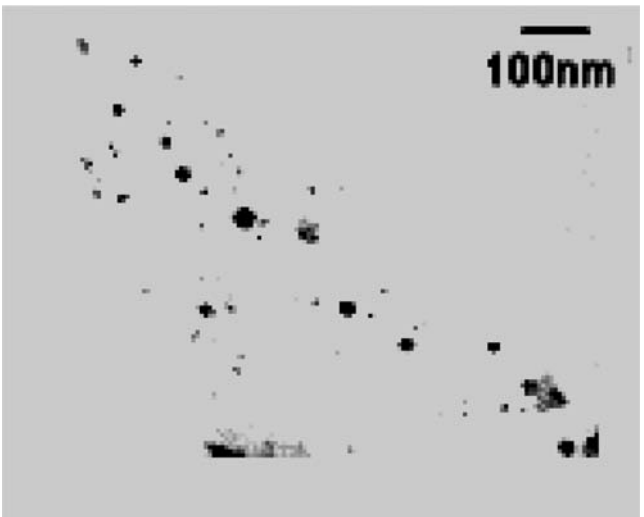

Fig. 7 TEM image of PU/(TiO_2–SiO_2) hybrid films ([NCO]/[OH]= 1.3/1.0 mol/mol; APTS/(TiO_2–SiO_2)=2 wt%; toluene=70 wt%; 4 h; 85 °C)

transformation of TiO_2 at 500 °C and then immigrated into the SiO_2 networks to form new Ti–O–Si bonds. It also confirms the existence of Ti–O–Si bonds in the composite nanoparticles.

FT-IR characterization

To gain better understanding of structure of composite nanoparticles and nanocompsites, we measured the FT-IR spectra of pure SiO_2 and TiO_2–SiO_2 composite nanoparticles, respectively (seen in Fig. 4). For pure SiO_2, the characteristic peaks of Si–O–Si are presented at wave numbers of 1,100, 805, and 475 cm^{-1}, respectively. For TiO_2–SiO_2 composite nanoparticles, the strength of characteristic peaks at wave numbers of 1,100, 805, and 475 cm^{-1} are reduced, respectively. Moreover, the new characteristic peak at a wave number of 940 cm^{-1} occurs in this case, indicating the formation of new Ti–O–Si bonds [2, 22, 23]. Figure 5 is the FT-IR spectra of TiO_2–SiO_2 composite nanoparticles, APTS-g–TiO_2–SiO_2 composite nanoparticles and TiO_2–SiO_2-g–PU hybrid particles. All the samples are washed by methanol. Figure 5a is the FT-IR spectrum of TiO_2–SiO_2 composite nanoparticles. In Fig. 5b, the characteristic peaks at wave numbers of 2,921 and 1,500 cm^{-1} are attributed to the characteristic peak of $–CH_2$ and the characteristic peak of $–NH_2$ at the wave number of 1,200 cm^{-1}, respectively [24, 25], meaning that the APTS-coupling agent has been successfully grafted onto the TiO_2–SiO_2 composite nanoparticle surface. In Fig. 5c, the characteristic peaks at wave numbers of 1,600, 1,530, 1,450, and 1,413 cm^{-1} are corresponding to the characteristic peaks of $–CH_2$, while the characteristic peak at the wave number of 1,723 cm^{-1} is a characteristic peak of C=O. In addition, the characteristic peaks of TiO_2–SiO_2-g–PU hybrid particles at 2,921, 1,458, and 1,226 cm^{-1} became sharper than those of APTS-g–TiO_2–SiO_2 composite nanoparticles, respectively, indicating that PU has been successfully grafted onto TiO_2–SiO_2 composite nanoparticles.

TGA analysis

The TGA curves in N_2 of pure PU and PU/(TiO_2–SiO_2) hybrids are presented in Fig. 6. It is obviously indicated that the initial thermal decomposition temperature of the PU/(TiO_2–SiO_2) hybrids is higher than that of the pure PU. For pure PU, the decomposition occurs at 262–404 °C, while in Fig. 6b, the decomposition of PU/(TiO_2–SiO_2) hybrids occurs at 272–415 °C. These results may be attributed to the strong interaction between the polymer chains and inorganic particles and consequently preventing the PU from thermal decomposition. Furthermore, the thermal stability of the hybrids is enhanced by the introduction of TiO_2–SiO_2 composite nanoparticles into the PU matrix [26].

TEM characterization

We investigated the morphology of PU/(TiO_2–SiO_2) hybrid films by TEM. The morphology of PU/(TiO_2–SiO_2) hybrid films could be observed in the TEM image. Figure 7 shows that the average particle size of TiO_2–SiO_2 composite nanoparticles in PU/(TiO_2–SiO_2) hybrid films is about 70 nm. Furthermore, TiO_2–SiO_2 composite nanoparticles are well dispersed in hybrid films without any aggregation. It could be explained that the assembly of TiO_2–SiO_2 composite nanoparticles with the PU matrix allows nanoparticles to be stable in hybrids films without aggregation.

Conclusions

In this paper, TiO_2–SiO_2 composite nanoparticles were successfully prepared by a sol–gel process. The formation of new Ti–O–Si bonds in the TiO_2–SiO_2 composite nanoparticles has been proved by XRD and FT-IR. In the case of the assembly of APTS/(TiO_2–SiO_2) and PU/(TiO_2–SiO_2), structurally well-defined PU/(TiO_2–SiO_2) hybrid films can be successfully prepared by using inorganic TiO_2–SiO_2 nanoparticles as building blocks incorporated into the organic PU matrix. The results show that Ti–O–Si bonds existed in TiO_2–SiO_2 composite nanoparticles. The average particle size of the TiO_2–SiO_2 composite particles is about 38 nm when the molar ratio of Ti/Si reaches to1:1. Furthermore, FT-IR and TGA confirmed that APTS had been successfully grafted to the TiO_2–SiO_2 composite nanoparticles' surface. The TEM image shows that TiO_2–SiO_2 composite nanoparticles in PU/(TiO_2–SiO_2) hybrid films are still in nanoscale. The TGA results present that the thermal stability of PU/(TiO_2–SiO_2) hybrid films is higher than that of pure PU films.

Acknowledgment This work was supported by National Science Foundation of China (Grant no. 20606016,10676013, 20576053).

References

1. Du WC, Wang HT, Zhong W, Shen L, Du QG (2005) J Sol-Gel Sci Technol 34:227
2. Innocenzi P, Martucci A, Guglielmi, Armelao L, Pelli S, Righini GC, Battaglin GC (1999) J Non-Cryst Solids 259:182
3. Luis M, Liz M, Paul M (2003) J Phys Chem B 107:7312
4. Timothy VW, Timothy EP (2001) J Am Chem Soc 123:7497
5. Chen Q, Miyaji F, Kokubo T, Nakamura T (1999) Biomaterials 20:1127
6. Jeffrey P, Krzystof M (2001) Chem Mater 13:3436
7. Timothy VW, Timothy EP (2001) J Am Chem Soc 123:7497
8. Timothy VW, Timothy EP (1999) J Am Chem Soc 121:7409
9. Spange S (2000) Prog Polym Sci 25:781
10. Mark JE (1992) J Appl Polym Sci Appl Polym Symp 50:273
11. Schmidt H (1994) J Sol-Gel Sci Technol 1:217

12. Schmidt H, Kasemann R, Burkhart T, Wagner G, Arpac E, Geiter E (1995) ACS Symp Proc Ser 585:331
13. Betrabet SC, Wilkes GL (1994) J Inorg Organomet Polym 4:343
14. Hideki G, Curtis WF (2001) Chem Mater 13:2783
15. Takavuki N, Keiko N, Hiroki I, Shiqeru S, Kimio K (2005) In: 54th SPSJ Annual Meeting 2005-Polymer Preprints
16. Chen YC, Zhou SX, Yang HH, Wu LM (2006) J Sol-Gel Sci Technol 37:39
17. Chen TK, Tien YI, Wei KH (2000) Polymer 41:1345
18. Tortora M, Gorrasi G, Vittiria V, Gali G, Ritrovati S, Chiellini E (2002) Polymer 43:6147
19. Nunes RCR, Pereira RA, Fonseca JLC, Pereira MR (2001) Polym Test 20:707
20. Wei Y, Yang W, Tan H, Zhong YP (2004) Polyurethane Industry 19:17
21. Chen S, Sui JJ Chen L (2004) Colloid Polym Sci 283:66
22. Du XM, Almeida RM (1996) J Mater Res 11:353
23. Almeida RM, Christensen EE (1997) J Sol-Gel Sci Technol 8:409
24. Lu CL, Cui ZC, Guan C (2003) Macromol Mater Eng 288:717
25. Won BK, Sun HC, Lee JS (2000) J Phys Chem B 104:8670
26. Wang HT, Xu P, Shen M, Zhong W, Du QG (2006) Polym Degrad Stab 91:1455